

HELSINKI UNIVERSITY OF TECHNOLOGY
Faculty of Electronics, Communications and Automation
Department of Signal Processing and Acoustics

Vo Si Van

Image Compression Using Burrows-Wheeler Transform

Master's Thesis submitted in partial fulfillment of the requirements for the degree of
Master of Science in Technology

Espoo, 25.11. 2009

Supervisor:	Professor Jorma Skyttä
Instructor:	D.Sc (Tech.) Jan Eriksson

Author:	Vo Si Van	
Name of the thesis:	Image Compression Using Burrows-Wheeler Transform	
Date:	25.11. 2009	Number of Pages: 8+57
Faculty:	Electronics, Communications and Automation	
Professorship:	S-88 Signal Processing in Telecommunications	
Supervisor	Professor Jorma Skyttä	
Instructor:	D.Sc (Tech.) Jan Eriksson	
<p>The purpose of this thesis was to study image compression using the Burrows-Wheeler transform. The aim of image compression is to compress the image into a format which saves the storage space and provides an efficient format for transmission via telecommunication channels. The Burrows-Wheeler transform is based on block sorting, which rearranges data into an easier format for compressing.</p> <p>Before utilizing the Burrows-Wheeler transform, the image need to be pre-process by using a discrete cosine transform, a discrete wavelet transform or predictive coding. Then the image is converted from a 2-dimensional to a 1-dimensional pixel sequence with different scanning methods. The forward Burrows-Wheeler transform is applied on block of the image data.</p> <p>While compressing the image into the smallest storage space, the move-to-front and run-length encoding can be used to improve the compression ratio before entropy encoding. This thesis studies both lossless and lossy image compression.</p>		
<p>Keywords: the Burrows-Wheeler transform, image compression, lossless and lossy compression</p>		

Tekijä:	Vo Si Van	
Työn nimi:	Image Compression Using Burrows-Wheeler Transform	
Päivämäärä:	25.11. 2009	Sivumäärä: 8+57
Tiedekunta:	Elektroniikka, Tietoliikenne ja Automaatio	
Professuuri:	S-88 Tietoliikenteen Signaalinkäsittely	
Työn valvoja:	Professori Jorma Skyttä	
Työn ohjaaja:	TkT Jan Eriksson	
<p>Tämän työn tarkoituksena on tutkia kuvan pakkausta Burrows-Wheelerin muunnosta käyttämällä. Kuvan tiivistämisessä tarkoituksena on tiivistää kuva muotoon, joka tallennettaessa saatetaan mahdollisimman pieneen tilaan, sekä nopeuttaa kuvan siirtämistä tietoliikenteen välityksellä. Burrows-Wheeler muunnos perustuu annettuun datan uudelleenjärjestämiseen, niin että muunnoksen jälkeen data on helpompi pakata.</p> <p>Ennen kuin voidaan käyttää Burrows-Wheelerin muunnosta, kuva pitäisi ensin esikäsitellä diskreettillä kosinimuunnoksella, diskreettillä aallokemuunnosella tai ennustuskoodauksella. Tämän jälkeen 2D-kuvan pikselit skannataan käyttämällä esilaisia skannausmenetelmiä, ja voidaan hyödyntää Burrows-Wheelerin menetelmällä.</p> <p>Burrows-Wheelerin yhteydessä käytetään hyväksi esim. move-to-front ja run-length-koodaus menetelmiä ennen varsinaista entropiakoodausta, jotta kuva voitaisiin tiivistää mahdollisimman pieneen tilaan. Työssä tutkitaan sekä häviöllistä että häviötöntä kuvan pakkausta.</p>		
Avainsanat: Burrows-Wheeler muunnos, kuvanpakkaus, häviöllinen-, häviötön pakkaus.		

Acknowledgements

I wish to thank my instructor Dr. Jan Eriksson for his guidance and advice and professor Jorma Skyttä for supervising and commenting on this thesis.

I would also like to thank all my friends, especially Hannele, for her supports and discussions during my study at Helsinki University of Technology and during this work.

Special thanks are due to William Martin from Faculty of Electronics, Communications and Automation, Helsinki university of Technology, for reviewing my thesis, and his constructive feedback and comments.

Lastly, I want to express my warmest gratitude to my parents, my brother, my sisters, my daughter Thao Mai and the rest of my family, for their love, support, motivation and for standing by me through my educational career.

Vantaa, 25.11. 2009

Vo Si Van

Contents

List of Abbreviations	vii
List of Notations	viii
Chapter 1: Introduction	1
1.1 Thesis Organization.....	2
Chapter 2: Basic of Image Compression	2
2.1 Digital Image.....	2
2.2 Information Theory.....	3
2.3 Data Redundancy.....	4
2.3.1 Coding Redundancy.....	5
2.3.2 Interpixel Redundancy.....	6
2.3.3 Psychovisual Redundancy.....	6
2.4 Felicity Criteria.....	7
2.5 Data Compression.....	8
2.5.1 Lossless Image Compression.....	9
2.5.2 Lossy Image Compression.....	10
Chapter 3: Digital Image Processing	11
3.1 Discrete Cosine Transform (DCT).....	12
3.2 Discrete Wavelet Transform (DWT).....	15
3.3 Lossless Predictive Coding.....	18
3.4 Lossy Predictive Coding.....	19
3.5 Quantization Block Size.....	21

3.6 Entropy Encoding	22
3.6.1 Huffman Coding.....	22
3.6.2 Arithmetic Coding.....	23
Chapter 4: Burrows-Wheeler Compression	25
4.1 The forward transform.....	26
4.2 The reverse Burrows-Wheeler Transform.....	27
4.3 Variant of the Burrows-Wheeler Transform	28
4.3.1 Lexical Permutation Sorting.....	28
4.4 Pre and post processing	29
4.4.1 Path Scanning	30
4.4.2 Move-To-Front.....	34
4.4.3 Inversion Frequencies.....	35
4.4.4 Distance Coding	36
4.4.5 Run–Length Encoding.....	37
Chapter 5: Experimental results.....	39
5.1 Experimental Data	39
5.2 Explaining Given Methods.....	40
5.3 Experimental Result using Discrete Cosine Transform	40
5.3.1 Comparison with Different Methods.....	40
5.3.2 Effect of Scanning Paths	41
5.3.3 Effect of Block Sizes	42
5.4 Effect of Different Threshold in DWT	45
5.5 Experimental Result using Predictive Coding.....	46
5.5.1 Effect of Scanning Paths on Predictive Coding	48
Chapter 6: Conclusions.....	50
References	53
Appendix A	56

List of Abbreviations

RGB	Red, Blue, Green
BWT	Burrows-Wheeler Transform
DCT	Discrete Cosine Transform
DM	Delta Modulation
DPCM	Differential Pulse Code Modulation
DWT	Discrete Wavelet Transform
IF	Inversion Frequencies
MTF	Move-To-Front
RLE	Run-length-Encoding
RH	Raster Horizontal Scan
RV	Raster Vertical Scan
SH	Snake Horizontal Scan
SV	Snake Horizontal Scan
SS	Spiral Scan
VSS	Vertical Spiral Scan
JPEG	Joint Photographic Experts Group

List of Notations

$f(x, y)$	Original image
$\hat{f}(x, y)$	Reconstructed image
$e(x, y)$	Error between images
e_{rms}	Root-mean square error
SNR_{rms}	Mean-square signal-to-noise ratio
$F(u, v)$	Discrete Cosine Transform
$Q(u, v)$	Quantizer step-size parameter
$F_q(u, v)$	Quantization of discrete cosine transform
$\varphi(x, y)$	Scaling function
$\psi(x, y)$	Basic function of wavelet
$W_\varphi(j_0, m, n)$	Discrete wavelet transform of function $f(x, y)$
$T(t, x)$	Hard or soft threshold
$Q[e_n]$	Quantizer of DPCM

Chapter 1: Introduction

The aim of this Master's thesis is to study the Burrows-Wheeler Transform [7] for use in image compression; the purpose is to compress images into the smallest space as possible. The Burrows-Wheeler transform (BWT) is a data compression algorithm, which was presented for the first time in 1994 by Burrows and Wheeler. The main idea is to achieve better data compression ratio to save storage space and to allow faster data transmission via different networks. The BWT based compression is close to the best known algorithm for text data nowadays, it could also perhaps be used to improve the compression performance of images. This thesis studies the BWT method for image compression and also some variants of the BWT method. The BWT is applied in combination with other additional methods of image compression techniques, for example, with move-to-front and run-length encoding, as well as with different scanning path methods and tested with various block sizes to get the competitive result for image compression. The results are obtained by testing empirically the pre-processing methods such as discrete cosine transform (DCT), discrete wavelet transform (DWT) and predictive coding. This thesis will set the JPEG image compression standard as a basic target for comparison to our methods.

There are many types of data, for example, sound, text, video and image that could benefit in some way from applying the BWT for compression purposes. The scope of this Master's thesis, however, concentrates on working with still image data.

1.1 Thesis Organization

In Chapter 2, the basic idea of image compression is introduced: the general concepts related to digital images and information theory including the measurement methods between images. Few transformation techniques such as DCT, DWT and Predictive coding for pre-processing of digital image data are introduced in Chapter 3. There are two important entropy coding techniques: *Huffman* and the *Arithmetic* coding. Predictive coding is also discussed from the perspective of lossless and lossy methods. Chapter 4 shows several techniques for converting the 2-dimensional image into 1-dimensional sequence. In this thesis, the zig-zag, Hilbert, raster, snake, and spiral scans are used for linearization of the 2-dimensional image. The Burrows-Wheeler Transform (BWT) is presented along with few techniques to improve the efficient in image compression. Chapter 5 shows the experimental results and the analysis parts of this thesis, which is the core of this thesis investigation. Finally, in Chapter 6, conclusions of this thesis are presented and suggestions are made for possible areas of further study.

Chapter 2: Basic of Image Compression

This chapter begins with an introduction about the representation of the digital image, the mathematics of lossless and lossy image compression, and presents the basic elements of an image. Then some fundamental concepts of information theory such as average the amount of data and entropy are discussed. After this, three data redundancies are shown briefly to give the reader a better understanding of the concept of *compression ratio*, which is important in image compression. And finally, some fidelity criteria classes showing the calculation of compressed image data are presented and the signal-to-noise ratio is used to compare the original image with the compressed image.

2.1 Digital Image

A digital image is represented by a two-dimensional array of picture elements (or pixels), which are arranged in rows and columns. A digital image can be presented as an $M \times N$ matrix [4]

$$f(x, y) = \begin{bmatrix} f(0,0) & f(0,1) & \cdots & f(0,N-1) \\ f(1,0) & f(1,1) & \cdots & f(1,N-1) \\ \vdots & \vdots & \ddots & \vdots \\ f(M-1,0) & f(M-1,1) & \cdots & f(M-1,N-1) \end{bmatrix}, \quad (2.1)$$

where $f(0,0)$ gives the pixel of the first row and the first column of the image and $f(M-1, N-1)$ defines the M^{th} row and N^{th} column of the image. A Grey-scale image, also referred to as a monochrome image contains the values ranging from 0 and 255, where 0 is black, 255 is white and values in between are shades of grey.

In a color digital image, each pixel of the image is represented by three different color channels, usually red, green and blue, shortly *RGB*. Each R, G and B is also in the range of 0 and 255 and each pixel is represented in three bytes, except in a Grey-scale image is represented only by one byte, which, naturally, makes the storage space of color images three times the size of Gray-scale images. The color image can be represented in *pixel-interleaved* or a *color-interleaved* format. In a pixel-interleaved format, each image pixel is represented by three color values. In a color-interleaved format, the color is represented by three different color matrices, one for each color channel [20].

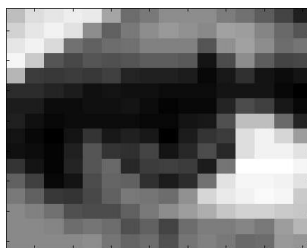


Figure 1: 36×36 grey scale image of human eye

2.2 Information Theory

One of the most important features in the field of information theory is entropy, which was introduced by C. E. Shannon in 1948 in his paper *A Mathematical Theory of*

Communication. In Shannon's theory, entropy is the quantitative measure of information, choice and uncertainty [22]. Suppose an image contains pixels referred to as the symbols, r_0, r_1, \dots, r_k and the each symbol has a probability of its occurrence $p(r_0), p(r_1), \dots, p(r_k)$. The amount of information for each symbol is defined as $-\log_2 p(r_k)$, and, thus, is usually expressed in *bits*. Applying the previous definition, the entropy is defined as follows. The entropy $H(S)$ is the average amount of information, in other words, the entropy is the average number of bits needed for coding an image pixel,

$$H(S) = - \sum_{k=0}^{L-1} p(r_k) \log_2 p(r_k) \quad (2.2)$$

2.3 Data Redundancy

Data redundancy is a central issue in digital image compression. Because transmission bandwidth and space storage are limited, at the same time, the aim is to maximum amount of data within those constraints. To solve this problem by removing information that is *redundant*. Data with redundancy can be compressed; on the other hand, data without any redundancy can not be compressed. The idea is to reduce or remove the redundant information contained within data. Suppose n_1 and n_2 are two units of a set of data representing the same information. The compression ratio, C_R , is denoted as [4]

$$C_R = \frac{n_1}{n_2} \quad (2.3)$$

The relative Redundancy R_D of the data set, n_1 , is defined as

$$R_D = 1 - \frac{1}{C_R} \quad (2.4)$$

There are three types of redundancies to explore in image compression and coding techniques:

- Coding Redundancy
- Interpixel Redundancy
- Psychovisual Redundancy

Coding redundancy and interpixel redundancy can be explored by lossless image compression. Psychovisual redundancy can be explored by lossy image compression.

2.3.1 Coding Redundancy

Image compression reduces the amount of data required to describe a digital image by removing the redundant data in the image, because in image data, some pixel values occur more common than others. Lossless image compression deals with reducing coding redundancy. A variable length coding is commonly used for coding redundancy reduction, where the average number of bits used per pixel in the image is reduced [10]. For example, *Huffman* and *arithmetic* coding are techniques which explore coding redundancy using in image compression to reduce or to remove the redundant data from the image. Coding redundancy utilizes histogram analysis to construct codes to reduce the amount of data used in the image representation [9].

$$p_r(r_k) = \frac{n_k}{n} \quad k = 0, 1, 2, \dots, L-1 \quad (2.5)$$

The average length of the number of bits used to represent each pixel is

$$L_{avg} = \sum_{k=0}^{L-1} l(r_k) p_r(r_k) \quad (2.6)$$

where $l(r_k)$ is the length of the codeword used in pixel r_k and $p_r(r_k)$ is the occurrence probability of each r_k . The total codeword length used in image $M \times N$ is $M \times N \times L_{avg}$ [4].

2.3.2 Interpixel Redundancy

The interpixel redundancy technique which is related to interpixel correlation within the image is another form of data redundancy. The values of the neighboring pixels of image are usually highly correlated to each other. The grey levels of pixels are usually similar to neighboring pixels. Thus, the values of pixels can be predicted or approximated from examining the neighboring pixels: it is said that the image contains interpixel redundancy. Interpixel redundancy is reversible, thus the reconstructed image can be exactly the same as the original image. For example, predictive coding and run-length coding techniques will reduce the interpixel redundancies efficiently.

2.3.3 Psychovisual Redundancy

It is known that the human eye does not respond to all visual information with equal sensitivity, some information being more important than other information [10]. The psychovisual redundant image data can be reduced or removed without changing the visual quality of the image [11]. This type of reduction is referred to as *quantization*. Since some information is lost, however, the process is not reversible. Therefore, this compression technique is known as *lossy*. The end result of applying these techniques is a compressed image file, whose size and quality are smaller than the original information, but whose resulting quality is still acceptable for the application at hand [24].

2.4 Felicity Criteria

In lossy compression methods, there will be some information loss during these methods. Thus, a reconstructed image may not be identical to the original image. Felicity Criteria are used for lossy image compression to measure the difference between the reconstructed images compared to the original image. There are two different Felicity Criteria classes: *Objective* felicity criteria and *subjective* felicity criteria. Below are two definitions of objective felicity criteria, where $f(x, y)$ presents an original image, and $\hat{f}(x, y)$ is the approximation of original image. The difference of the original image and the reconstructed image is given as [4]

$$e(x, y) = \hat{f}(x, y) - f(x, y). \quad (2.7)$$

The root mean-square error between the original image and the reconstructed image is defined as

$$e_{ms} = \left[\frac{1}{MN} \sum_y \sum_x [e(x, y)]^2 \right]^{1/2}, \quad (2.8)$$

the Mean-square signal-to-noise ratio between original image $f(x, y)$, and the reconstructed $\hat{f}(x, y)$ is

$$SNR_{ms} = \frac{\sum_y \sum_x \hat{f}(x, y)^2}{\sum_y \sum_x [e(x, y)]^2}. \quad (2.9)$$

Although objective felicity criteria offer a simply and convenient mechanism for evaluating information loss, most decompressed images ultimately are viewed by humans. Subjective felicity criteria shows how the quality of the image is measured depends on the number of human observers. This is done by showing the evaluators a sample image of the original image and the reconstructed image using the absolute

rating scale for their average evaluations. The absolute rating scale can be used side-by-side, which compares the images within the scale of $\{-3, -2, -1, 0, 1, 2, 3\}$ to represent the subjective evaluations $\{\textit{much worse}, \textit{worse}, \textit{slightly worse}, \textit{the same}, \textit{slightly better}, \textit{better}, \textit{much better}\}$, another example rating scale for the quality of the sample image could be a scale from 1- 6, with 1 standing for “excellent” and 6 standing for “unusable”. [4][16]

2.5 Data Compression

In data compression, the main idea is to convert the original data into a new data form, which contains the same information but can use a smaller space for storing the data. This is very important for saving expensive data storage space and for achieving a faster data transmission ratio. As mentioned earlier, data compression can be divided into lossless and lossy compression techniques presented briefly in the next sub-section. The compression system model consists of two important parts, which are an *encoder* and a *decoder*. At the encoder block, the original image $f(x, y)$ is converted into another representation, which can be transferred through the channel to the receivers. When reading the data, compressed data has to be uncompressed at the receiver side using a decoder block.. In the lossless compression method, $f(x, y)$ and $\hat{f}(x, y)$ are actually the same but in the lossy compression method, the reconstructed images contain some error, and the images are not equal.

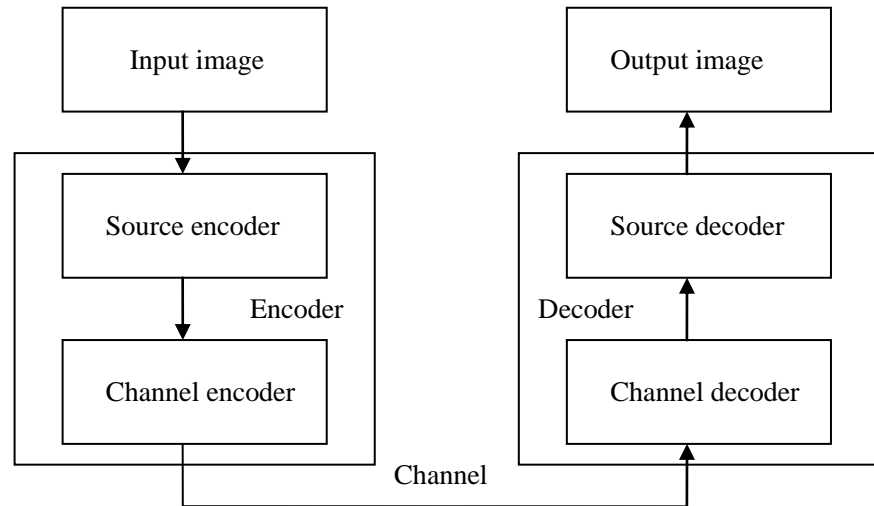


Figure 2: A general compression system model

Figure 2 shows the compression system model for the image. The original input image is pre-processing in encoder block, where the result of the image is a 1-dimensional bit stream sequence. Then the sequence is transmitted via different telecommunication channels to decoder block, where the sequence of data is decoded. After transmission over the *channel*, the encoded representation is fed to the decoder, where a reconstructed output image is generated. In general, the output image may or may not be an exact replica of input image [4].

2.5.1 Lossless Image Compression

In lossless image compression methods, when the images have been compressed with some specific methods, the original images can be reconstructed from the compressed images without losing any information, that is

$$f(x, y) = \hat{f}(x, y), \quad (2.10)$$

where $f(x, y)$ denotes the original image and $\hat{f}(x, y)$ is the reconstructed image.

Lossless compression methods are also known as reversible because of this lossless feature. Besides using the lossless compression methods for images, it is widely used

also for text compression, where it is important that the original text data can be recovered exactly from the compressed data [2]. The disadvantage is that the compression ratio is not so high, precisely because no data is lost. For instance, lossless compression is generally the technique of choice for text files, where losing words data could cause a problem.

2.5.2 Lossy Image Compression

Using lossy image compression methods will always yield some loss of information. In lossy compression images can not be reconstructed exactly to their original form, that is

$$f(x, y) \neq \hat{f}(x, y). \quad (2.11)$$

This is because of some small errors of information are introduced into the original image. The lossy methods usually compress images to a smaller size than any known lossless methods, thus achieving a higher compression ratio. Lossy compression is usually used in applications where a slight loss of information does not cause any harm. This is why lossy compression is commonly used to compress videos, images and sound, where small errors may be acceptable, and the idea only is to loose information that would not be detected by most human users. In the next chapter, lossy image compression methods using with discrete cosine transform, wavelet transform, and lossy predictive coding are presented.

Chapter 3: Digital Image Processing

In this chapter, the aim is to give an overview of different image processing methods, for example, discrete transformation and quantization using for image processing. The idea of transform coding is to map pixels of an image into the format such that the pixels are less correlated compared to the original image. The transform is a lossless method, since while doing the inverse transform there is no loss of information. The transform coding focuses the energy only on a few important elements, and quantizes those elements which have less important information, in lossy coding. There are many different transform methods for image compression, however, in this thesis the *discrete cosine transform* (DCT) and *discrete wavelet transform* (DWT) methods are utilized. For image processing, it is also possible to use predictive coding that predicts the following pixels of image instant of a transformation. The following step in image processing is quantization, which makes the transform coding and predictive coding to be lossy. During the quantization step, the majority of the less important coefficients are quantized to zero by applying the quantization table. In subsection (3.5) is showing the idea of obtaining different size of quantization table. In the end of this chapter, two entropy encoding methods, *Huffman and Arithmetic* coding, are presented.

3.1 Discrete Cosine Transform (DCT)

Discrete cosine transform is one of the most used transformation techniques in image compression. The idea of DCT is to decorrelate the image data by converting the image into elementary frequency components. By using DCT-based coding, the digitized image needs to be split into blocks of pixels, typically 8×8 blocks. The DCT scheme itself is lossless, but it can also be said that the DCT technique is a *near-lossless* compression technique, because of the rounding of pixel values. A quantization step, where the process will produce a lot of zero coefficients for better compression ratio could be applied here, but there is some loss of information during this step. The forward discrete cosine transform of a 2-dimensional 8×8 block image is given as follows

$$F(u, v) = \frac{1}{4} C(u)C(v) \sum_{x=0}^7 \sum_{y=0}^7 f(x, y) \cos \frac{(2i+1)u\pi}{16} \cos \frac{(2j+1)v\pi}{16} \quad (3.1)$$

The forward discrete cosine transform concentrates the energy on low frequency elements, which are located in the top-left corner of the subimage. Following equation (3.2) is inverse cosine transform (IDCT) using for decoding the compressed image defined as [1]

$$f(x, y) = \frac{1}{4} \sum_{u=0}^7 \sum_{v=0}^7 C(u)C(v) F(u, v) \cos \frac{(2i+1)u\pi}{16} \cos \frac{(2j+1)v\pi}{16}, \quad (3.2)$$

where

$$C(u)C(v) = \begin{cases} \frac{1}{\sqrt{2}} & u, v=0 \\ 1 & otherwise \end{cases}, \quad (3.3)$$

$F(u, v)$ is the transformed DCT coefficient and $f(x, y)$ is the value of the pixel of the original sample of the block [1].

As an example, consider using the discrete cosine transform to an original image of size 256×256 pixels. First the image is split into 8×8 pixel blocks, as an example consider

$$f(x, y) = \begin{pmatrix} 49 & 57 & 34 & 31 & 33 & 28 & 14 & 29 \\ 20 & 24 & 21 & 20 & 17 & 16 & 18 & 22 \\ 19 & 20 & 22 & 16 & 12 & 14 & 14 & 35 \\ 17 & 18 & 16 & 15 & 13 & 22 & 25 & 68 \\ 47 & 27 & 32 & 26 & 7 & 28 & 46 & 54 \\ 71 & 46 & 45 & 60 & 24 & 38 & 65 & 37 \\ 70 & 86 & 37 & 52 & 57 & 53 & 29 & 96 \\ 66 & 84 & 80 & 44 & 29 & 40 & 93 & 175 \end{pmatrix} \quad (3.4)$$

After shifting the pixels of the $f(x, y)$ matrix by -128 pixel levels to yield pixel values between $[-128, 127]$, it is then cosine transformed by forward DCT using the equation (Eq. 3.1). Note that, large values, also called the lower frequencies, are now concentrated in the top-left corner of the matrix and the higher frequencies are in the bottom-right corner.

$$F(u, v) = \begin{pmatrix} -709 & -11 & 78 & -40 & 17 & -13 & 5 & -17 \\ -131 & 28 & -53 & 30 & -9 & 2 & 0 & 6 \\ 76 & 10 & 18 & -19 & 3 & -30 & -5 & -1 \\ 9 & 45 & -26 & 38 & -4 & 23 & -10 & -6 \\ 21 & -27 & 34 & -25 & -3 & -5 & 9 & 5 \\ 4 & 11 & -12 & 13 & 16 & -33 & 0 & -14 \\ 12 & 5 & 4 & -7 & -10 & 25 & -2 & 8 \\ -2 & 11 & 1 & 5 & 3 & -14 & 5 & -3 \end{pmatrix} \quad (3.5)$$

DCT transformation is said to be near-lossless, because Equation 3.5 is already rounded to the nearest integer.

Now the 64 DCT coefficients are ready for quantization. Each of the DCT coefficients $F(u, v)$ are divided by the *JPEG* quantization table $Q(u, v)$, and then rounded to the nearest integer [4]

$$F_q(u, v) = \text{Round}\left(\frac{F(u, v)}{Q(u, v)}\right), \quad (3.6)$$

where $Q(u, v)$ is defined as

$$Q(u, v) = \begin{pmatrix} 16 & 11 & 10 & 16 & 24 & 40 & 51 & 61 \\ 12 & 12 & 14 & 19 & 26 & 58 & 60 & 55 \\ 14 & 13 & 16 & 24 & 40 & 57 & 69 & 56 \\ 14 & 17 & 22 & 29 & 51 & 87 & 80 & 62 \\ 18 & 22 & 37 & 56 & 68 & 109 & 103 & 77 \\ 24 & 35 & 55 & 64 & 81 & 104 & 113 & 92 \\ 49 & 64 & 78 & 87 & 103 & 121 & 120 & 101 \\ 72 & 92 & 95 & 98 & 112 & 100 & 103 & 99 \end{pmatrix} \quad (3.7)$$

The table $Q(u, v)$ is called a JPEG standard quantization table. The quantization step is mainly a lossy operation; the resulting matrix contains many zero-values at the higher frequency components, which can be seen in the following matrix

$$F_q(u, v) = \begin{pmatrix} -44 & -1 & 8 & -3 & 1 & 0 & 0 & 0 \\ -11 & 2 & -4 & 2 & 0 & 0 & 0 & 0 \\ 5 & 1 & 1 & -1 & 0 & -1 & 0 & 0 \\ 1 & 3 & -1 & 1 & 0 & 1 & 0 & 0 \\ 1 & -1 & 1 & 0 & 0 & 0 & 0 & 0 \\ 0 & 0 & 0 & 0 & 0 & 0 & 0 & 0 \\ 0 & 0 & 0 & 0 & 0 & 1 & 0 & 0 \\ 0 & 0 & 0 & 0 & 0 & 0 & 0 & 0 \end{pmatrix} \quad (3.8)$$

After de-quantization, the inverse discrete cosine transform is used yielding in to the following matrix, also known as the reconstructed matrix of the original image:

$$\hat{f}(x, y) = \begin{pmatrix} 49 & 56 & 31 & 21 & 39 & 24 & 8 & 34 \\ 23 & 30 & 27 & 26 & 28 & 14 & 8 & 25 \\ 12 & 5 & 17 & 25 & 10 & 9 & 26 & 35 \\ 32 & 4 & 15 & 23 & 1 & 16 & 53 & 55 \\ 59 & 25 & 29 & 35 & 14 & 26 & 55 & 51 \\ 68 & 52 & 52 & 52 & 34 & 41 & 45 & 50 \\ 67 & 76 & 68 & 52 & 42 & 36 & 58 & 100 \\ 66 & 90 & 71 & 40 & 36 & 40 & 85 & 167 \end{pmatrix} \quad (3.9)$$

By comparing the 8×8 subimage $f(x, y)$ and $\hat{f}(x, y)$, the difference of the original and the reconstructed image is given by

$$e(x, y) = \hat{f}(x, y) - f(x, y). \quad (3.9) - (3.4)$$

Obviously there are slight differences between these matrices, because of the quantization step applied after forward DCT.

3.2 Discrete Wavelet Transform (DWT)

Discrete wavelet transform (DWT) is one of the most effective methods in image compression. DWT transforms a discrete time signal into a discrete wavelet representation by splitting frequency band of image in difference subbands. In 2-dimensional DWT, it is first necessary to apply 1-dimensional DWT in each row of the image before applying one-dimensional column-wise to produce the final result [36]. Four subband images named as LL , LH , HL and HH , are created from the original image. LL is the subband containing lowest frequency, which is located in the top left corner of the image and other three are subbands with higher frequencies. In a 2-dimensional image signal in wavelet transform, it is containing one *scaling function*, $\varphi(x, y)$, and three 2-dimensional *wavelet* $\psi^H(x, y)$, $\psi^V(x, y)$, $\psi^D(x, y)$, are required.

Each is a product of a one-dimensional scaling function φ and corresponding wavelet ψ [4]. The definition of scaling function is defined as

$$\varphi(x, y) = \varphi(x)\varphi(y) \quad (3.10)$$

There are three different basic functions of the wavelet: $\psi^H(x, y)$ is for the horizontal, $\psi^V(x, y)$ for the vertical and $\psi^D(x, y)$ for the diagonal subband. Wavelets are defined as

$$\begin{aligned} \psi^H(x, y) &= \psi(x)\varphi(y) \\ \psi^V(x, y) &= \varphi(x)\psi(y) \\ \psi^D(x, y) &= \psi(x)\psi(y) \end{aligned} \quad (3.11)$$

The discrete wavelet transform of function $f(x, y)$ of the size $M \times N$ is then given by [4]

$$W_\varphi(j_0, m, n) = \frac{1}{\sqrt{MN}} \sum_{x=0}^{M-1} \sum_{y=0}^{N-1} f(x, y)\varphi_{j_0, m, n}(x, y) \quad (3.12)$$

$$W_\psi^i(j, m, n) = \frac{1}{\sqrt{MN}} \sum_{x=0}^{M-1} \sum_{y=0}^{N-1} f(x, y)\psi^i_{j, m, n}(x, y) . \quad (3.13)$$

Figure 3 shows four quarter-size output subimages, which are denoted as $W_\varphi, W_\psi^H, W_\psi^V$ and W_ψ^D

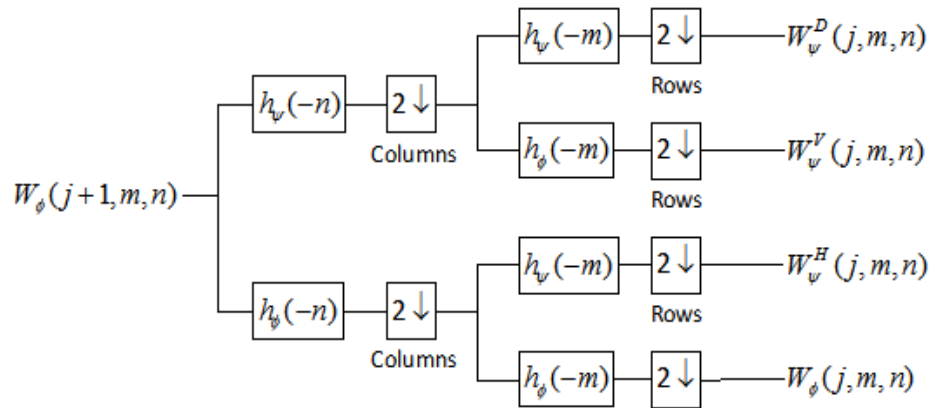


Figure 3: Discrete Wavelet Transform [4]

The top-left corner subimage is almost the same as the original image, due to the energy of an image being usually distributed around the lower band. A top-left corner subimage is called the approximation and others are the details [12][13].

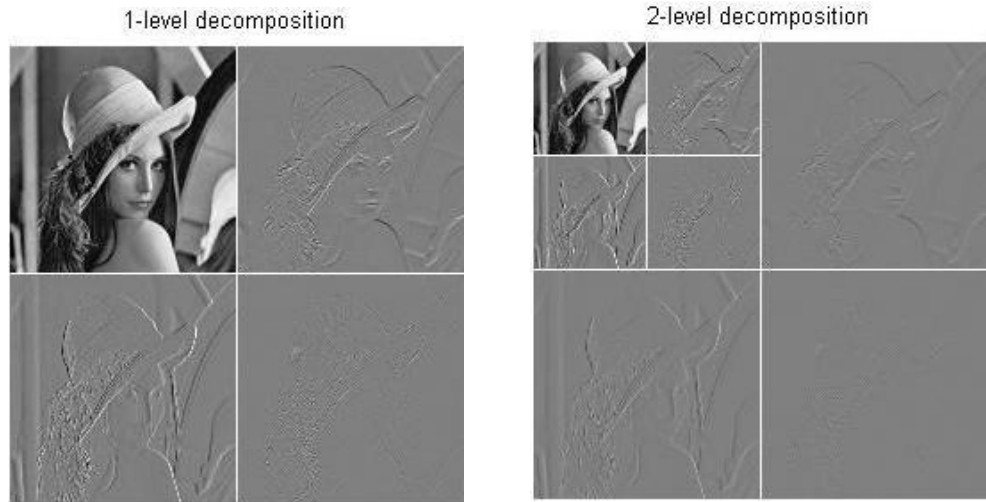


Figure 4: 1-level and 2-level decomposition of WT

Figure 4 shows the discrete wavelet of the 1-level and the 2-level decomposition using discrete wavelet transform. The 1-level decomposition has four subimages, where the most important sub-image is located at top-left corner of the image. For the 2-level decomposition, the final image consists of seven subimages.

The quantization step of the wavelet is also referred to as thresholding. Hard threshold and soft threshold are two different threshold types used in image compression. In the hard threshold technique, if the value of the coefficient is less than the defined value of threshold, then the coefficient is scaled to zero, otherwise the value of the coefficient is maintained as it is. That is [20],

$$T(t, x) = \begin{cases} 0 & \text{if } |x| < t \\ x & \text{otherwise} \end{cases} \quad (3.14)$$

In the soft threshold technique, if the value of the coefficient is less than the defined value of the threshold, then the coefficient is scaled to zero, otherwise the value of the

coefficient is reduced by the amount of the defined value of the threshold. Note that a threshold is set only for the detail coefficients [15]. The soft threshold is given by

$$T(t, x) = \begin{cases} 0 & \text{if } |x| < t \\ \text{sign}(x)(|x| - t) & \text{otherwise} \end{cases}. \quad (3.15)$$

3.3 Lossless Predictive Coding

Predictive coding is a technique used to predict the future values of the image pixels based on pixels already received. The aim is to reduce the interpixel redundancy. In lossless predictive coding, is based on eliminating the interpixel redundancies of closely spaced by extracting and coding only the new information in each pixel. The new information of the pixel is defined as the difference between the actual and predicted value of that pixel [4]. The difference between the actual and the predicted value of that pixel, e_n , also referred to as *prediction error*. The prediction error is the subtraction of the original image pixel values and predicted pixels

$$e_n = f_n - \hat{f}_n. \quad (3.16)$$

The encoder of the lossless predictive coding system consists of a *predictor*.

$$\hat{f}_n = \text{round}[\sum_{i=1}^m \alpha_i f_{n-i}] \quad (3.17)$$

f_n is defined as original image and \hat{f}_n denotes a predicted pixel which is rounded to the nearest integer. The system model of the encoder for lossless predictive coding is shown in Figure 5. The model contains the identical predictor and the prediction error for encoding.

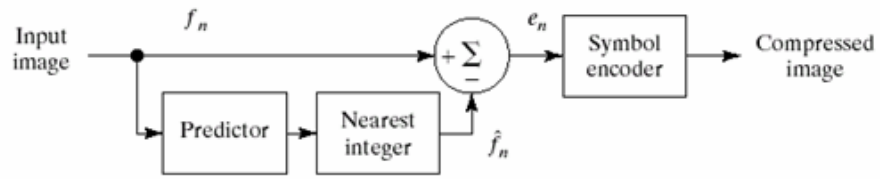


Figure 5: Lossless Predictive coding system model [4]

Here are examples of the first and the second orders of our predictor in the 2-dimensional model used in this thesis [4]

$$\begin{aligned} \hat{f}(x, y) &= f(x, y - 1) + f(x - 1, y) \\ \hat{f}(x, y) &= 0.5f(x, y - 1) + 0.5f(x - 1, y) \end{aligned} \tag{3.18}$$

The predictive error images using the original images are shown below with the first and the second order predictor applied

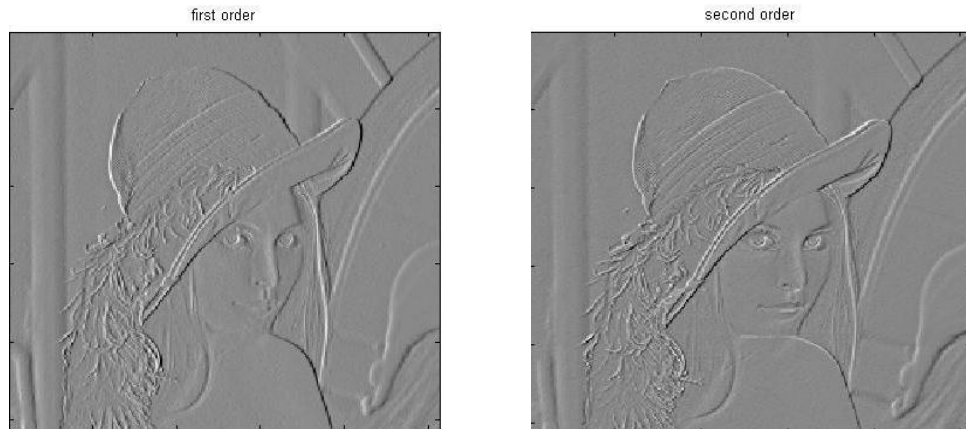


Figure 6: The first and the second order predictive error

3.4 Lossy Predictive Coding

A general system model of an encoder for lossy predictive coding is shown in Figure 7, which is consisting of a *quantizer*, *identical predictor* and the output of the system also referred as the *prediction error*

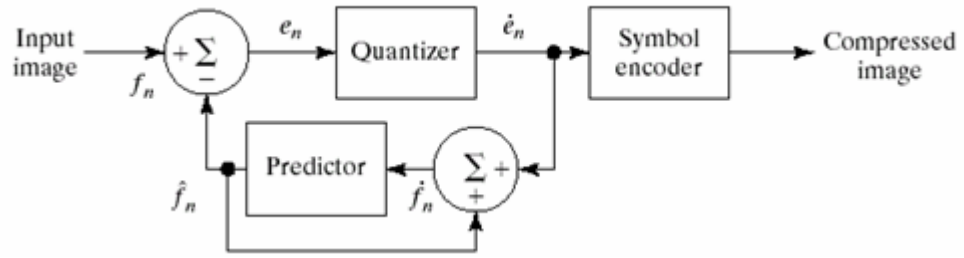


Figure 7: Lossy predictive coding system model [16]

Differential pulse code modulation (DPCM) is one of the most commonly used lossy predictive coding techniques for image compression. The idea of DPCM is to predict the value of the neighboring pixels, which are highly correlated to each other, utilizing the identical predictor of the system. The difference between the original pixel and the predicted pixel, referred to as an error pixel, is then quantized and encoded [19]. For lossy predictive coding, we applied the same prediction error and the predictors used in the lossless predictive coding. The difference of the original image and the predicted image to referred as the prediction error e_n , is defined as

$$e_n = f_n - \hat{f}_n, \quad (3.19)$$

and the predictor $\hat{f}(x, y)_1$ is denoted as a first order predictor and $\hat{f}(x, y)_2$ is the second order predictor

$$\begin{aligned} \hat{f}(x, y)_1 &= f(x, y-1) + f(x-1, y) \\ \hat{f}(x, y)_2 &= 0.5f(x, y-1) + 0.5f(x-1, y) \end{aligned} \quad (3.20)$$

The example quantizer of the DPCM can be defined as

$$\tilde{e}_n = Q[e_n] = 16 * \left\lfloor \frac{255 + e_n}{16} \right\rfloor - 256 + 8 \quad (3.21)$$

The other well known form of lossy predictive coding is *Delta Modulation* (DM), which is a simplified version of DPCM, the quantizer being defined as [4]

$$\tilde{e}_n = \begin{cases} +\xi & \text{for } e_n > 0 \\ -\xi & \text{otherwise} \end{cases} \quad (3.22)$$

The output of the quantized error is then encoded using *Huffman* or *Arithmetic* coding.

3.5 Quantization Block Size

In JPEG, each block of 8×8 samples is independently transformed using the two-dimensional discrete cosine transform. This is a compromise between contrasting requirements; larger blocks would provide higher coding efficiency, whereas smaller blocks limit complexity. The 8×8 discrete cosine transform coefficients of each block have to be quantized before entropy coding [26]. But the question remains, what if we want to divide the image data into a different block size, such as 2×2 , 4×4 , 16×16 , 32×32 or 64×64 ? The quantization table must be able to process in the same size as image block size, which is able to quantize.

$$Q(u, v) = \begin{pmatrix} 16 & 11 & 10 & 16 & 24 & 40 & 51 & 61 \\ 12 & 12 & 14 & 19 & 26 & 58 & 60 & 55 \\ 14 & 13 & 16 & 24 & 40 & 57 & 69 & 56 \\ 14 & 17 & 22 & 29 & 51 & 87 & 80 & 62 \\ 18 & 22 & 37 & 56 & 68 & 109 & 103 & 77 \\ 24 & 35 & 55 & 64 & 81 & 104 & 113 & 92 \\ 49 & 64 & 78 & 87 & 103 & 121 & 120 & 101 \\ 72 & 92 & 95 & 98 & 112 & 100 & 103 & 99 \end{pmatrix}$$

When reducing the quantization matrix $Q_{8 \times 8}(u, v)$ into the $Q_{4 \times 4}(u, v)$ block size, it can be done easily by dividing the matrix into 4×4 blocks, and then average the four values in each block. On the other hand, the interpolation of the quantization matrix $Q_{8 \times 8}(u, v)$ can be simply done by expanding the matrix to $Q_{16 \times 16}(u, v)$, then the resulted matrix is interpolated to $Q_{32 \times 32}(u, v)$ or $Q_{64 \times 64}(u, v)$ quantization matrices.

3.6 Entropy Encoding

In this thesis entropy encoding is used for compression of image pixels after scanning the pixels into a 1-dimensional sequence. The aim of entropy encoding is to compress the image data into less memory space for storage, which also makes it easier to transmit the image data. Huffman coding and Arithmetic coding are the two most widely used entropy encoding methods [18].

3.6.1 Huffman Coding

Huffman coding is a data compression technique which has been used also in image compression. Huffman coding is based on the probabilities of the data occurring in the sequence. Symbols which occur more frequently will need fewer bits than symbols with less frequency. Consider we have a pixel symbol sequence consisting of 6 pixels; the probability of occurrence pixels are shown in Figure 8.

Original source		Source reduction			
Symbol	Probability	1	2	3	4
a_2	0.4	0.4	0.4	0.4	0.6
a_6	0.3	0.3	0.3	0.3	0.4
a_1	0.1	0.1	0.2	0.3	
a_4	0.1	0.1	0.1		
a_3	0.06	0.1			
a_5	0.04				

Figure 8: Huffman Coding [4]

First, Huffman code sums together the two lowest probability pixels into a new pixel with a new probability ($0.06+0.04=0.1$), repeating this until there is only one pixel, and the probability is 1. The reverse step to code each probability with binary code starts with the smallest source and works back to the original source. Given the binary 0 and 1 to the source on the right, then go backward with the same path, adding to the source 0

and 1. The operation is repeated for each reduced source until the original source is reached. The final code appears on the far left of Figure 9.

Original source			Source reduction			
Sym.	Prob.	Code	1	2	3	4
a_2	0.4	1	0.4 1	0.4 1	0.4 1	0.6 0
a_6	0.3	00	0.3 00	0.3 00	0.3 00	0.4 1
a_1	0.1	011	0.1 011	0.2 010	0.3 01	
a_4	0.1	0100	0.1 0100	0.1 011		
a_3	0.06	01010	0.1 0101			
a_5	0.04	01011				

Figure 9: Huffman Coding reverse [4]

As can be seen from Figure 9, the symbol a_2 gives only the code with only 1 bit, and the a_5 has the code with 5 bits. In other words, the symbols that occur more frequently are coded with fewer bits than those symbols with least frequency.

3.6.2 Arithmetic Coding

Arithmetic coding [4] is another entropy coding technique. Like in Huffman coding, the occurrence probabilities of the symbols in the encoding message needs to be known in Arithmetic coding. Arithmetic coding encodes the data by creating a real number between 0 and 1 representing the value sequence. For ease of understanding, let us encode a sequence, $a_1a_2a_3a_3a_4$ with probabilities given in Figure 10. In arithmetic coding, the process starts with an interval [0, 1), all symbols have their occurrence probability and are set into a subinterval of the frequency at which it occupies in the message. Because the first symbol of the message being coded, the message interval is initially narrowed to [0.0, 0.2). The next step is to divide message interval again into smaller subinterval for the next symbol, a_2 , yielding a subinterval [0.04, 0.08). For the next symbol, a_3 , the interval is divided into a new subinterval, producing [0.056,

0.072). By continuing this, we will arrive at the final interval [0.0688, 0.06752). The sequence of symbols can be coded with any number within the interval representing the data.

Source Symbol	Probability	Initial Subinterval
a_1	0.2	[0.0, 0.2)
a_2	0.2	[0.2, 0.4)
a_3	0.4	[0.4, 0.8)
a_4	0.2	[0.8, 1.0)

Figure 10: Probabilities and the Initial Subinterval of symbol

Figure 10 shows four symbol of source and the probability of each symbol, as well as the initial subinterval of which symbol is associated. Figure 11 shows the basic process of arithmetic coding. There are five symbol of message and four symbol of source is coded.

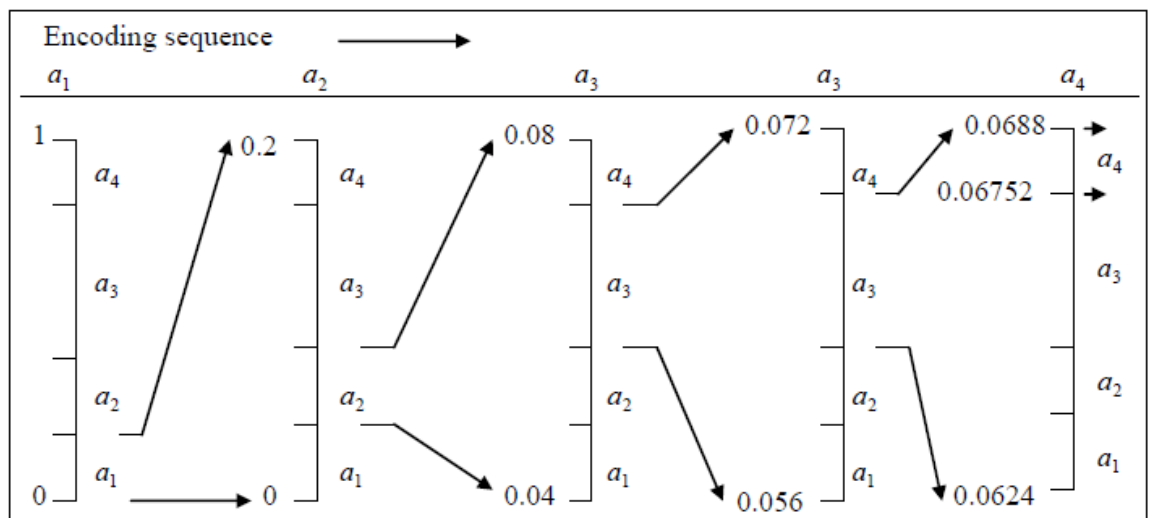


Figure 11: Arithmetic Coding [4]

Chapter 4: Burrows-Wheeler Compression

The Burrows-Wheeler transform is based on the block-sorting lossless data compression algorithms [7] which are used in many practical applications, especially in data compression. The BWT transforms a block of data into a form, which is easier to compress. The BWT is widely used in text data, but also is rapidly becoming popular in image data compression. In this thesis, we applied the discrete wavelet transform (DWT), discrete cosine transform (DCT) and predictive coding methods before using the Burrows-Wheeler transformation to achieve the better compression rate of the image. One-dimensional sequences of pixels are obtained by path scanning; two-dimensional transformed image is converted into a one-dimensional sequence of pixels by using zigzag, Hilbert path filling or raster scanning methods. The Burrows-Wheeler transformation is then applied for the sequence transform it to an easier form for compression. In this chapter, BWT is defined, and some pre and post processing methods are discussed. The move-to-front, inversion frequencies, distance coding and run-length-encoding methods are used after the BWT to obtain better compression performance in image compression.

4.1 The forward transform

Consider a 1-dimensional pixel sequence obtained by path scanning

$$p = [3 \ 2 \ 5 \ 3 \ 1 \ 4 \ 2 \ 6]$$

The original sequence p is copied to the first row, also referred to as *index* 0. The sequence is then sorted with all left-cyclic permutations into each next *index* row. The step 1 of the BWT is presented in Table 1.

Table 1: Step 1 of BWT

<i>index</i>	Step 1
0	3 2 5 3 1 4 2 6
1	2 5 3 1 4 2 6 3
2	5 3 1 4 2 6 3 2
3	3 1 4 2 6 3 2 5
4	1 4 2 6 3 2 5 3
5	4 2 6 3 2 5 3 1
6	2 6 3 2 5 3 1 4
7	6 3 2 5 3 1 4 2

Next rows are sorted lexicographically. The step 2 of the BWT is shown in Table 2. Step 3 is the final step of the BWT process consisting of output of the BWT and the final index.

Table 2: Step 2 and 3 of BWT

<i>index</i>	Step 2	<i>index</i>	Step3
0	1 4 2 6 3 2 5 3	0	3
1	2 5 3 1 4 2 6 3	1	3
2	2 6 3 2 5 3 1 4	2	4
3	3 1 4 2 6 3 2 5	3	5
4	3 2 5 3 1 4 2 6	4	6
5	4 2 6 3 2 5 2 1	5	1
6	5 3 1 4 2 6 3 2	6	2
7	6 3 2 5 3 1 4 2	7	2

The original sequence $p = [3 \ 2 \ 5 \ 3 \ 1 \ 4 \ 2 \ 6]$ appears in the fifth row of Table 2, and the output of the BWT transform is the last column, indicated by $L = [3 \ 3 \ 4 \ 5 \ 6 \ 1 \ 2 \ 2]^T$,

with the $index = 4$. The result can be written as $BWT = [index, L]$, where L is the output of the Burrows-Wheeler transform and $index$ describes the location of the original sequence in the lexicographically ordered sequence. For later on we also utilize the first column $F = [1\ 2\ 2\ 3\ 3\ 4\ 5\ 6]^T$, which can be obtain from L by sorting to perform the reverse transform of the BWT. Obviously there are some repetitions of pixels at the transformed form of the output sequence.

4.2 The reverse Burrows-Wheeler Transform

The BWT is a reversible transformation which can recover the original sequence from the BWT output sequence. In reverse transform only the BWT output sequence L and $index$ are needed for reconstructing the original sequence. To solve the reverse BWT using output of the BWT L and $index$, the reverse BWT is presented in Table 3.

Here $BWT^{(-1)}[index, 3\ 3\ 4\ 5\ 6\ 1\ 2\ 2] = [3\ 2\ 5\ 3\ 1\ 4\ 2\ 6]$.

Table Construction: For $i=1 \dots n-1$,

Step $(3i-2)$: Place column n in front of column $1 \dots i-1$.

Step $(3i-1)$: Order the resulting length i strings lexicographically.

Step $3i$: Place the ordered list in the first i columns of the table.

Table 3: Reverse BWT- transform modified form [6]

$index$	$(i=1)$			$(i=2)$			$(i=3)$		
	a	b	c	a	b	c	a	b	c
0	3	1	1...3	31	14	14...3	314	142	142...3
1	3	2	2...3	32	25	25...3	325	253	253...3
2	4	2	2...4	42	26	26...4	426	263	263...4
3	5	3	3...5	53	31	31...5	531	314	314...5
4	6	3	3...6	63	32	32...6	632	325	325...6
5	1	4	4...1	14	42	42...1	142	426	426...1
6	2	5	5...2	25	53	53...2	253	531	531...2
7	2	6	6...2	26	63	63...2	263	632	632...2

<i>index</i>	<i>(i=4)</i>			<i>(i=5)</i>			<i>(i=6)</i>		
	<i>a</i>	<i>b</i>	<i>c</i>	<i>a</i>	<i>b</i>	<i>c</i>	<i>a</i>	<i>b</i>	<i>c</i>
0	3142	1426	1426...3	31426	14263	14263...3	314263	142632	142632...3
1	3253	2531	2531...3	32531	25314	25314...3	325314	253142	253142...3
2	4263	2632	2632...4	42632	26325	26325...4	426325	263253	263253...4
3	5314	3142	3142...5	53142	31426	31426...5	531426	314263	314263...5
4	6325	3253	3253...6	63253	32531	32531...6	632531	325314	325314...6
5	1426	4263	4263...1	14263	42632	42632...1	142632	426325	426325...1
6	2531	5314	5314...2	25314	53142	53142...2	253142	531426	531426...2
7	2632	6325	6325...2	26325	63253	63253...2	263253	632531	632531...2

<i>index</i>	<i>(i=7)</i>		
	<i>a</i>	<i>b</i>	<i>c</i>
0	3142632	1426325	1426325...3
1	3253142	2531426	2531426...3
2	4263253	2632531	2632531...4
3	5314263	3142632	3142632...5
4	6325314	3253142	3253142...6
5	1426325	4263253	4263253...1
6	2531426	5314263	5314263...2
7	2632531	6325314	6325314...2

The output of the reverse transform is also at the *index 4*, which is why the *index* is utilized to represent the output of the forward transform and the sequence is $[3\ 2\ 5\ 3\ 1\ 4\ 2\ 6]$, which is the same as the original sequence p .

4.3 Variant of the Burrows-Wheeler Transform

Since publication of the Burrows-Wheeler transform in the early 1990s, many extensions and variants of the original BWT have been developed for the aim of possibly getting even better compression ratio. In this thesis, we only show briefly on the idea level of one variant of BWT; Lexical permutation sorting.

4.3.1 Lexical Permutation Sorting

The lexical permutation sorting is a variant of the traditional Burrows-Wheeler Transform, which was developed for the first time by Arnavut and Magliveras [8]. In

the traditionally BWT, the pair of index and the last column of the lexically ordered ($index, L$) of the matrix are transmitted. In lexical permutation sorting any other columns of the lexically ordered can be selected and recovered into the original sequence without yielding any error. In the studies of Arnavut and Magliveras, it has been shown that it is possible to select any of the other columns and still recover the data [3].

Let us recall the sequence $p = [3\ 2\ 5\ 3\ 1\ 4\ 2\ 6]$, the sequence first sorted by cyclic permutations, then is ordered lexically similarly in the BWT. The difference of lexical permutation sorting compared to the traditional forward BWT is the selection of the output column of the matrix shown below. Instead of selecting the last column, any other columns can be selected, for example, choosing the second column $S = [4\ 5\ 6\ 1\ 2\ 2\ 3\ 3]^T$ to be transmitted.

Table 4: Lexical permutation sorting

<i>index</i>	Step 1	<i>index</i>	Step 2
0	1 4 2 6 3 2 5 3	0	4
1	2 5 3 1 4 2 6 3	1	5
2	2 6 3 2 5 3 1 4	2	6
3	3 1 4 2 6 3 2 5	3	1
4	3 2 5 3 1 4 2 6	4	2
5	4 2 6 3 2 5 2 1	5	2
6	5 3 1 4 2 6 3 2	6	3
7	6 3 2 5 3 1 4 2	7	3

4.4 Pre and post processing

In this section several techniques, which could be used to pre and post process the Burrows-Wheeler transform to obtain better image data performance, are introduced. Path scanning is a process which is done before using the BWT to convert the 2-

dimensional data into a 1-dimensional form. After using the BWT the data could be post processed by using several methods such as move-to-front and run-length-encoding for easier image entropy coding.

4.4.1 Path Scanning

Because the Burrows-Wheeler transformation only works with sequential data, the image data first needs to be convert from a 2-dimensional to a 1-dimensional pixel sequence. Considering the $N \times N$ image, the result of path scanning is the form of $1 \times N^2$. There are various scanning techniques for scanning the pixels of the image. In this chapter we use several typical techniques for reading the pixels for later Burrows-Wheeler transformation.

4.4.1.1 Zig-Zag Scan

Zig-Zag scans the image along the anti-diagonals beginning with the top-most anti-diagonal. Each anti-diagonal is scanned from the left top corner to the right bottom corner [6]. The result of the 2-dimentional image using a zig-zag scan yields a coefficient ordering sequence which is $ZigZag = (1, 2, 5, 9, 6, 3, 4, 7, 10, 13, 14, 11, 8, 12, 15, 16)$.

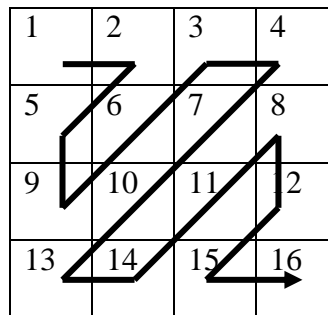


Figure 12: Zig-zag scan

4.4.1.2 Hilbert Scan

The Hilbert curve method scans every pixel of the image in the square image with any size of $2^k \times 2^k$ [6]. The Hilbert curve has a basic element of a square with one open side, referred to as a subcurve [6]. The open side of the subcurve can be top, bottom, left and right. Each subcurve has two end-points, and each of these can be the “entry” point of the “exit” point. A first level Hilbert curve is just a single curve. The second level Hilbert curve replaces that with four smaller curves, which can inter-connected with each others by three joins yielding a second level Hilbert curve. Every next level repeats the process or replacing each subcurve by four smaller subcurves and three joins

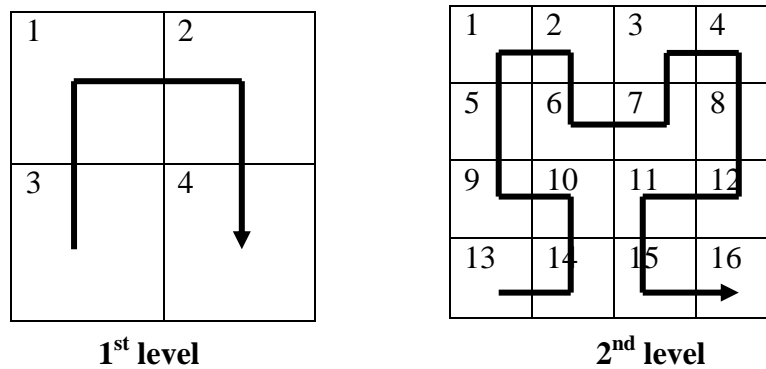


Figure 13: 1st and 2nd level of the Hilbert Scan

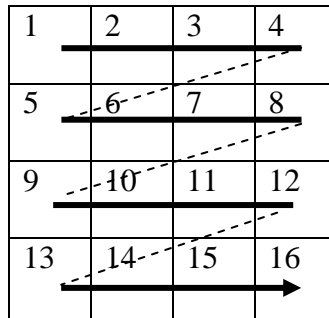
4.4.1.3 Raster Scan

A raster horizontal scan is the simplest scanning technique where the image is scanned row by row from top to bottom and from left to right within each row [6]. The result of the raster horizontal scan of the 2-dimensional image of size 4×4 is $RH = (1,2,3,4,5,6,7,8,9,10,11,12,13,14,15,16)$.

The raster vertical (RV) scans in a way similar to RH, but vertically; the image is scanned column by column from left to right and from top to bottom within each

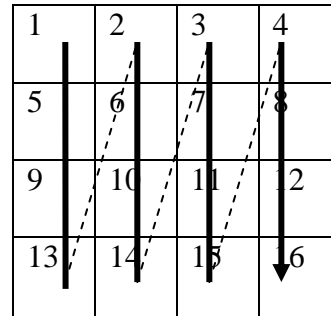
column [6]. The result of the raster vertical scan performed on the 2-dimensional image is $RV = (1,5,9,13,2,6,10,14,3,7,11,15,4,8,12,16)$.

Raster horizontal scan:



RH

Raster vertical scan:



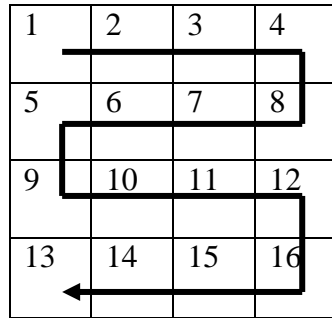
VH

Figure 14: Raster scan

In snake horizontal scan (SH), the image is scanned row by row starting from the top left corner pixel going through to the right, scanning to the end of the first row, and continue scanning the next row starting from the right to the left pixel. This is a variant of the raster horizontal scan method described above [6]. The result of snake horizontal scan of the 2-dimensional image is $SH = (1,2,3,4,8,7,6,5,9,10,11,12,16,15,14,13)$.

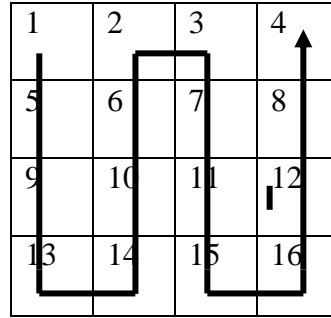
In snake vertical scan (SV), the image is scanned column by column starting from the top left corner pixel going to the end of the column, continuing with scanning the next column by starting from the bottom to the top pixel. This is a variant of the raster vertical scan method described above [6]. The result of the snake horizontal scan of the example image is $SV = (1,5,9,13,14,10,6,2,3,7,11,15,16,12,8,4)$.

Snake horizontal scan



SH

Snake vertical scan



SV

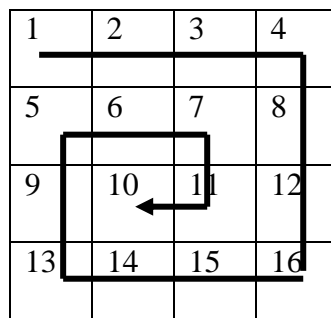
Figure 15: Snake scan

4.4.1.4 Spiral-Scan

In spiral scan (SS), the image is scanned from the outside to the inside, beginning from the left top corner of the image. The result of the spiral scan performed on the 2-dimensional image is $SS = (1,2,3,4,8,12,16,15,14,13,9,5,6,7,11,10)$.

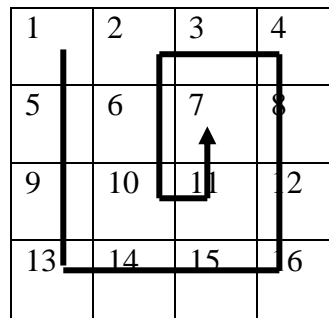
The vertical spiral scan is a variants of the spiral scan, with the image being scanned from the outside to the inside, beginning from the left top corner of the image, scanning vertically to the bottom. The result of the spiral scan of the 2-dimentional image is $VSS = (1,5,9,10,14,15,16,12,8,4,3,2,6,10,11,7)$.

Spiral scan



SS

Vertical spiral scan



VSS

Figure 16: Spiral scan

4.4.2 Move-To-Front

The *move-to-front transform* (MTF) is an encoding of data designed to improve performance of entropy encoding techniques of compression. The move-to-front is a process that is usually used after Burrows-Wheeler transformation to ranking the symbols according to their relative frequency. Move-to-front is base on a dynamic alphabet kept in a move-to-front list, where the current character during scanning is always moved to beginning of the alphabet [25]. After processing MTF, the sequence is as long as the original sequence because it does not compress the original sequence. The main idea is to achieve a better compression performance in entropy coding.

Consider, the Burrows-Wheeler transforms output sequence is

$$L_0 = [3 \ 2 \ 4 \ 5 \ 7 \ 1 \ 2 \ 2].$$

Now we want to transform the sequence using MTF. First we need to initialize the index value list. In practice, the list is the order by byte value with 256 entries. In this case we have the list

$$l_0 = [0 \ 1 \ 2 \ 3 \ 4 \ 5 \ 6 \ 7]$$

The first pixel of the sequence is '3', which can be found in the fourth index of the list. We add the particular index to the Rank column, and then move the index to the front of the list, given

$$l_1 = [3 \ 0 \ 1 \ 2 \ 4 \ 5 \ 6 \ 7]$$

Table 5: Move-to-Front

Sequence	List	Rank
<u>3</u> 3 4 6 7 1 2 2	0 1 2 3 4 5 6 7	3
3 <u>3</u> 4 6 7 1 2 2	3 0 1 2 4 5 6 7	0
3 3 <u>4</u> 6 7 1 2 2	3 0 1 2 4 5 6 7	4
3 3 4 <u>6</u> 7 1 2 2	4 3 0 1 2 5 6 7	6
3 3 4 6 <u>7</u> 1 2 2	6 4 3 0 1 2 5 7	7
3 3 4 6 7 <u>1</u> 2 2	7 6 4 3 0 1 2 5	5
3 3 4 6 7 1 <u>2</u> 2	1 7 6 4 3 0 2 5	5
3 3 4 6 7 1 2 <u>2</u>	2 1 7 6 4 3 0 5	0

By doing this to the end of the sequence, the final output of rank is obtained

$$MTF = [3 \ 0 \ 4 \ 6 \ 7 \ 5 \ 5 \ 0]$$

From the result of Move-to-Front the Rank, a data sequence is containing a lot of symbol in the low integer range.

4.4.3 Inversion Frequencies

The inversion frequencies (IF) method was introduced by Arnavut and Magliveras [8], the aim being to replace the move-to-front stage. The idea of the inversion frequencies method is based on the distance between the occurrences of the symbols after the BWT stage [3]. For example, the sequence $L = [3 \ 2 \ 5 \ 1 \ 4 \ 1 \ 3 \ 4 \ 5 \ 6 \ 1 \ 2 \ 2]$ is the output of the BWT. The first step is to create a list of each symbol. Here we have a list of symbol $S = [1 \ 2 \ 3 \ 4 \ 5 \ 6]$. Starting with the first symbol of the list by counting the distance of the symbol then removes the symbol from the original sequence, and so on. For better understanding, let us look at the table below.

Table 6: Inversion Frequencies

List	Occurrence	Sequence
1	3, 1, 4	3 2 5 1 4 1 3 4 5 6 1 2 2
2	1, 6, 0	3 2 5 4 3 4 5 6 2 2
3	0, 2	3 5 4 3 4 5 6
4	1, 0	5 4 4 5 6
5	0, 0	5 5 6
6	0	6

The output of the inversion frequency is [3 1 4 1 6 0 0 2 1 0 0 0 0]. Compared to the original sequence, there are notably more zero-value created by the inversion frequencies method.

4.4.4 Distance Coding

Distance coding is based of the start of each symbol in the output of the BWT, thus we need to know the first occurrence of the symbol [3]. Then, we must count the distance of the same symbol from the first occurrence of the symbol. The symbol is counted from the original sequence without removing the symbols. The end of the symbol will get the distance of 0 to inform the end of each symbol. For example, $L = [3\ 2\ 5\ 1\ 4\ 1\ 3\ 4\ 5\ 6\ 1\ 2\ 2]$

Table 7: Distance Coding [3]

Symbol	First occurrence	Distance to the next run
1	4	2, 5, 0
2	2	10, 0
3	1	6, 0
4	5	3, 0
5	3	6, 0
6	10	0

When decoding, we first start with the first occurrence column, by setting the first occurrence of each symbol to its own position. From the Table 7 it can be seen, that the symbol 1 fist occurrence is in the 4th position, symbol 2 is in the 2nd position, symbol 3 in the 1st, and so on. Here the “*” is an unknown symbol.

3	2	5	1	4	*	*	*	*	6	*	*	*
---	---	---	---	---	---	---	---	---	---	---	---	---

The Distance of the next run column tells us the distance to the same symbol; the symbol 1 distance to the next run is 2. Put the second 1 at the position 6 and the next distance is 5 from the position 6, which is position 11.

3	2	5	1	4	1	*	*	*	6	1	*	*
---	---	---	---	---	---	---	---	---	---	---	---	---

After continuing this with all symbols, the final result of decoder of distance coding became the following sequence, which is the same as the original sequence $L = [3\ 2\ 5\ 1\ 4\ 1\ 3\ 4\ 5\ 6\ 1\ 2\ 2]$

3	2	5	1	4	1	3	4	5	6	1	2	2
---	---	---	---	---	---	---	---	---	---	---	---	---

4.4.5 Run–Length Encoding

The run-length encoding (RLE) is a simple compression technique, which can be used either before or after the BWT to reduce the number of runs in data sequence. RLE is more efficient when the sequence includes much data that is duplicated. The main idea of RLE is to count the runs that are repeated in the input data and replace the pixels with a different number of repetitions. For example, the one-dimensional sequence pixels of input data **1, 1, 1, 2, 2, 2, 3, 3, 3, 4, 4, 4, 4, 4, 4**, the pixel “1” has repeated with 3 times, and the pixel “2” has 4 repetitions, the values can represented as $(1,3), (2,4), \dots$. The sequence can be encoded by pairs of (value, repetition) to the end of the original data.

Input data: 1, 1, 1, 2, 2, 2, 3, 3, 3, 4, 4, 4, 4, 4, 4

Encoder: 1, 3, 2, 4, 3, 3, 4, 6

To decode the run-length, the first symbol of the encoder table is known by the value of the symbol, the second symbol is the repetition of such a value, which is 3 times that of the symbol 1.

Decoder: 1, 1, 1, X, X, X, X, X, X, X, X, X, X, X, X

While decoding to the end of the value, the output of the decoder will become exactly the same as the input data.

Output data: 1, 1, 1, 2, 2, 2, 3, 3, 3, 4, 4, 4, 4, 4, 4

RLE encoding will compress the pixels of the sequence efficiently with the pixels which contain three or more runs. But if the repetitions of runs are less than 2, there is no reducing compressed ratio of the sequence [17], [6].

Input data: 1, 1, 2, 3, 3, 4

Encoder: 1, 2, 2, 1, 3, 2, 4, 1

Chapter 5: Experimental results

This chapter shows the image compression experimental result of different methods, and comparisons of images are given for several methods. The results are tabled and also shown some of the reconstructed images recovered from the original image. The results are presented for three different image compression techniques, which are discrete cosine transform, discrete wavelet transform and predictive coding. Included are methods such as move-to-front, run-length encoding, as well as the Burrows-Wheeler transform, which has been discussed in previous chapters of the thesis. Also shown are the results of the effect of different scanning paths; zig-zag, Hilbert, raster and snake. The image comparisons also have been done for various block sizes. Huffman coding is the entropy encoding which is used to compress the image data. Comparisons between the Burrows-Wheeler transform methods and the JPEG standard is also considered.

5.1 Experimental Data

There are seven test images, which are used for test data – *GoldHill*, *Bridge*, *Boat*, *Barb*, *Birds*, *Airplane* and *Lena*.

5.2 Explaining Given Methods

There are some abbreviations of different methods shown in this subsection. Here are some abbreviations along with an explanation of what they stand for:

- a) JPEG: JPEG (*Joint Photographic Experts Group*) standard (Section 3.2)
- b) BM: Burrows-Wheeler transform and move-to-front (Section 4.4.2)
- c) BR: Burrows-Wheeler transform and run-length encoding (Section 4.4.5)
- d) BMR: Burrows-Wheeler transform, move-to-front and run-length encoding
- e) Zig-Zag: Zig-zag scanning path (Section 4.4.1.1)
- f) Hilbert: Hilbert scanning path (Section 4.4.1.2)
- g) Raster: Horizontal raster scanning path scans from the left to right and from top to bottom (Section 4.4.1.3)
- h) Snake: Horizontal snake scanning path starts from the left top corner (Section 4.4.1.3)
- i) DWT: Only discrete wavelet transform is used without BWT is applied (Section 3.3)
- j) Predictive: Only predictive coding is used without BWT is applied (Section 3.4)

5.3 Experimental Result using Discrete Cosine Transform

5.3.1 Comparison with Different Methods

This subsection contains an evaluation of the results by applying the discrete cosine transform. Variations of the Burrows-Wheeler transform are compared to the JPEG standard. The JPEG standard applies the DCT as a basic technique using the block size of 8x8. The DCT coefficients are scanned in zig-zag order, and coefficients are

encoding with RLE. These techniques are also applied in BM, BR and BMR to give better comparison for the simulation results.

Table 8 shows that the JPEG standard gives the compression ratio (see Eq. 2.3) of **28:1** on average, while Burrows-Wheeler transform with run length encoding gives a compression ratio of **30:1**. However, the move-to-front method gives over **29:1** on average. This suggests that, applying the BWT will yield a better result compared to the original JPEG standard.

Table 8: Comparison of JPEG with BM, BR and BMR

Method	GoldHill	Bridge	Boat	Barb	Birds	Airplane	Average
JPEG	24.45	26.34	23.54	31.03	36.90	29.25	28.58
BM	29.68	26.68	22.68	25.68	37.57	31.87	29.05
BR	29.07	26.74	26.19	28.78	34.91	34.05	29.96
BMR	27.39	24.08	20.94	23.40	34.27	31.50	26.92

5.3.2 Effect of Scanning Paths

To evaluate the effect of the different scanning paths used in the study method, we applied the block size 32×32 of the DCT, Burrows-Wheeler transform and run-length encoding to see the results of each scanning method. Zig-zag, Hilbert, horizontal raster and horizontal snake scanning methods are performed.

The order of encoding is

- DCT \Rightarrow Scanning path \Rightarrow BWT \Rightarrow RLE

The Table 9 shows that applying the zig-zag scanning path achieved the best compression ratio which is nearly **30:1**, while the Hilbert curve is worst, giving a compression ratio only on average **29:1**.

Table 9: Comparing scanning paths

Scan	GoldHill	Brigde	Boat	Barb	Birds	Airplane	Average
Zig-Zag	24.52	28.34	25.12	30.91	35.30	33.16	29.56
Hilbert	25.84	23.07	23.07	31.75	33.71	29.89	28.80
Raster	22.08	28.53	24.60	30.79	35.15	34.71	29.31
Snake	22.94	28.94	24.37	30.91	35.30	31.87	29.05

Most of higher frequency coefficients are converted into zeros after the forward discrete cosine transformation, which are in the right-bottom corner. The zig-zag is suitable for this situation to scans the sequence of zeros at the end, achieving higher entropy and run-length coding efficiency.

The difference in results of Table 8 and Table 9 is due to block size of process. In zig-zag scanning path is applied 32×32 , while in BR method the block size is only 8×8 .

5.3.3 Effect of Block Sizes

In the DCT, the image data is split into smaller block to pre-process the data. Generally, DCT is broken into 8×8 blocks of pixels. However, in our application, we also tried various block sizes. For comparing different block sizes in DCT, we apply six different block sizes: 2×2 , 4×4 , 8×8 , 16×16 , 32×32 and 64×64 . The DCT coefficients of the block are scanned using the zig-zag scan and JPEG standard quantization table (see section 3.3.1).

The order of encoding is following:

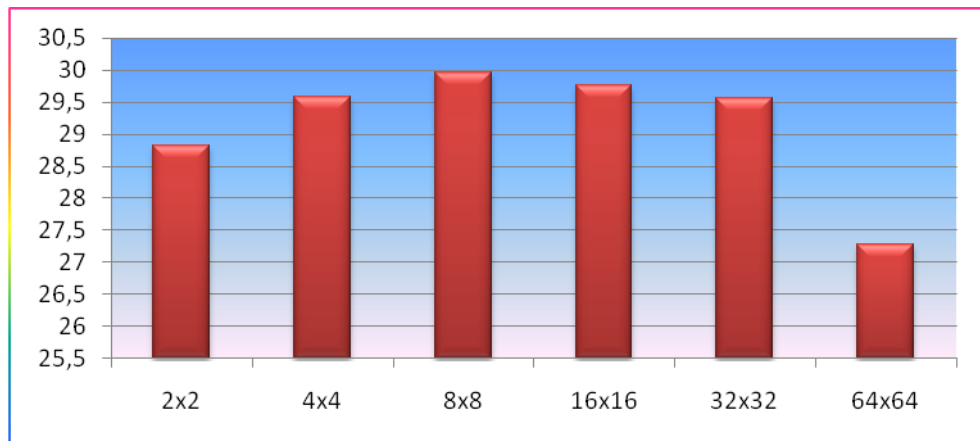
- DCT (block size) \Rightarrow Zig-Zag \Rightarrow BWT \Rightarrow RLE

Table 10: Comparing block sizes

Block size	GoldHill	Brigde	Boat	Barb	Birds	Airplane	Average
2×2	26.42	26.14	27.38	29.46	32.85	30.71	28.82
4×4	27.36	24.89	28.00	29.88	34.72	32.64	29.58
8×8	29.07	26.74	26.19	28.78	34.91	34.05	29.96
16×16	21.48	22.92	25.28	20.68	41.79	46.54	29.77
32×32	24.52	28.34	25.12	30.91	35.30	33.16	29.56
64×64	36.56	25.60	19.68	36.56	25.60	19.68	27.28

From the result shown in the Table 10, it is appear that the block size of 8×8 gives on average the best compression ratio, and the next best compression ratio is given by the block size of 16×16. The worst is the block size of 64×64. Also the block size of 2×2 and 4×4 give comparative result in this application. The conclusion of this subsection is that the small block size gives better result. However the smallest block size that could be used is 8x8.

The Figure 17 shows the compression ratio for each block size.

**Figure 17:** DCT with different block size

The Lena image with six different block size of DCT is shown in Figure 18. As can be observed, the reconstructed image with block size of 8×8 and 16×16 give it visually almost the same image. But with the block size of 2×2 and 64×64 give a poor reconstructed image because of the lower compression ratio shown in Table 10.



Figure 18: Lena with different blocks size of DCT

5.4 Effect of Different Threshold in DWT

In this part, we evaluate the results of different thresholds while using the discrete wavelet transform for lossy compression. There are three tested methods with three kinds of thresholds: 10, 30 and 50. In this application we have used Scale 1 decomposition and Scale 2 decomposition for the DWT. The block size of 64×64 is performed.

The orders of encodings are

- a) DWT \Rightarrow Threshold
- b) DWT \Rightarrow Threshold \Rightarrow BWT \Rightarrow MTF
- c) DWT \Rightarrow Threshold \Rightarrow BWT \Rightarrow RLE

Table 11a: Scale 1 decomposition with different threshold

Scale 1 Image	Threshold-10			Threshold-30			Threshold-50		
	DWT	BM	BR	DWT	BM	BR	DWT	BM	BR
GoldHill	23.18	19.97	20.18	28.59	21.52	20.72	32.86	22.53	23.22
Bridge	16.63	14.79	14.88	18.83	14.80	15.55	21.67	15.96	16.45
Boat	18.77	16.64	17.48	22.72	17.02	17.85	27.41	18.68	19.01
Barb	17.74	15.63	15.16	20.04	15.56	16.11	22.70	17.23	17.2
Birds	20.44	17.84	18.33	24.95	18.91	19.05	27.53	20.22	19.63
Airplane	16.79	15.91	14.96	18.77	16.79	16.04	21.96	17.27	16.54
Average	18.52	16.80	16.78	22.32	17.43	17.63	25.68	18.64	18.67

As can be seen from the result in Table 11a, in Scale 1 decomposition, applying the DWT without any use of Burrows-Wheeler transform will achieve the highest compression ratio. Obviously, the greater threshold gives the higher compression ratio compared to the smaller threshold. Here the threshold-50 gives a compression ratio of almost **26:1**, when threshold-10 gives only **18:1**. When comparing move-to-front and run-length-encoding with each other, in threshold-10 move-to-front is slightly better, but when the threshold is higher, run-length-encoding gives better results.

Table 11b: Scale 2 decomposition with different threshold

Scale 2	Threshold-10			Threshold-30			Threshold-50		
Image	DWT	BM	BR	DWT	BM	BR	DWT	BM	BR
GoldHill	36.81	25.96	31.02	54.24	30.91	32.83	74.64	37.06	34.78
Bridge	18.27	17.73	16.12	20.67	19.24	17.56	25.06	21.32	18.23
Boat	20.24	18.89	18.24	25.16	20.76	19.72	30.36	30.32	21.21
Barb	20.51	18.63	18.00	25.26	20.24	19.92	30.36	22.40	19.83
Birds	18.33	17.95	16.62	22.22	17.90	17.86	25.28	20.08	18.49
Airplane	22.72	20.90	19.90	26.50	22.42	21.74	33.50	24.14	22.39
Average	22.81	20.00	19.98	29.00	21.91	21.60	36.53	24.94	22.48

The results of Table 11b show that Scale 2 will give a much higher compression ratio compared to Scale 1 decomposition. Also, independent of the threshold, the move-to-front method yields a better ratio than the run-length encoding.

5.5 Experimental Result using Predictive Coding

This part of the thesis pre-processes the image data, and then compares it with different variants of the Burrow-Wheeler-transform, such as move-to-front, run-length-encoding and also a combination of these two methods. The zig-zag scanning order is applies in this technique after predictive coding.

By only using predictive coding without including any BWT methods, the compression ratio will be highest. The next best ratio is to apply the BWT and RLE. When applying the BWT, MTF and RLE together, the result is the lowest ratio.

Table 12: Predictive coding and different methods of BWT

Method	GoldHill	Bridge	Boat	Barb	Birds	Airplane	Average
Predictive	30.00	22.94	25.28	18.32	25.28	20.68	23.74
BM	14.60	13.04	14.296	10.07	12.92	11.40	12.72
BR	23.33	19.08	19.68	14.86	19.83	17.13	18.98
BMR	13.25	11.81	12.85	9.072	11.73	10.35	11.51

The results of Table 12 shows that the process of predictive coding before applying the Burrows-Wheeler transform yields a great gap between different methods. The compression ratio of BMR is only **11:1**, but the predictive coding is almost 24:1.

The predictive coding can be done also after the Burrows-Wheeler transform, but in this situation predictive coding must do the scanning for the image data to one-dimensional sequence data, instead of doing the path scanning after predictive coding.

- a) path scanning \Rightarrow BWT \Rightarrow Predictive
- b) path scanning \Rightarrow BWT \Rightarrow Predictive \Rightarrow move-to-front
- c) path scanning \Rightarrow BWT \Rightarrow Predictive \Rightarrow RLE
- d) path scanning \Rightarrow BWT \Rightarrow Predictive \Rightarrow move-to-front + RLE

Above the predictive coding is processed for the two-dimensional image data, now the predictive coding must be done for the 1-dimensional data.

Table 13: Predictive coding after BWT

Method	GoldHill	Bridge	Boat	Barb	Birds	Airplane	Average
BWT+Predictive	21.03	20.42	20.79	19.34	15.95	19.36	19.48
BWT+M	10.43	11.26	10.65	10.48	9.76	10.95	10.58
BWT+R	17.21	18.00	16.64	16.76	12.90	15.50	16.16
BWT+MR	9.59	10.25	9.71	9.57	8.98	10.03	9.68

The result of Table 13 gives poorer compression ratio compared to Table 12. So, when compressing the image using predictive coding after the BWT will give smaller ratio than applying the BWT before predictive coding. The worst case is using move-to-front together with run-length-encoding, its compression ratio is only near 10:1. Figure 19 shows that using the predictive coding before BWT will achieve higher compression ratio than after BWT.

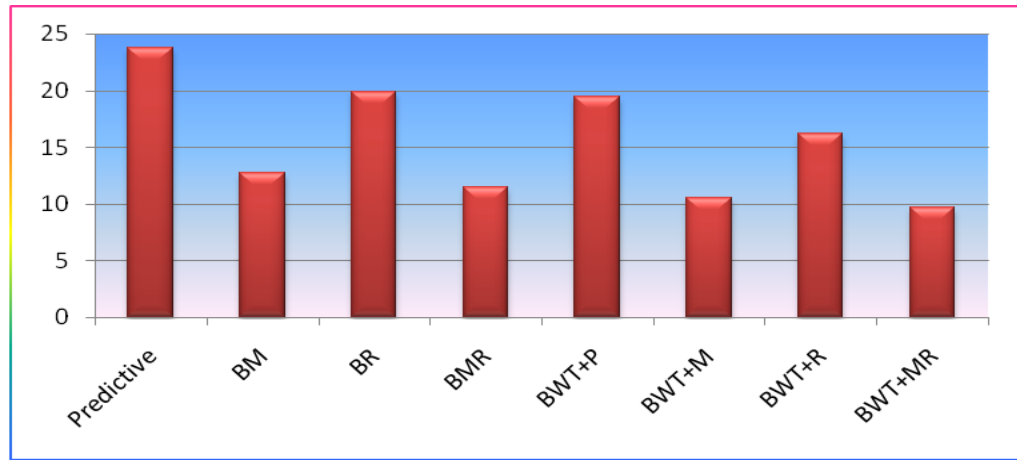


Figure 19: Predictive coding before and after BWT

As can be seen at Figure 19, the use of the Burrows-Wheeler transform before predictive (BWT+P) will achieve quite good compression ratio compared to the use of the Burrows-Wheeler transform before run-length encoding (BWT+R). The applying of the Burrows-Wheeler transform gave worst compression ratio.

5.5.1 Effect of Scanning Paths on Predictive Coding

To compare different scanning path, here we also apply the same scanning paths as before: zig-zag, Hilbert, Raster and Snake.

The phase of using predictive coding for the scanning path is the following:

- Predictive Coding \Rightarrow Scanning path \Rightarrow BWT \Rightarrow RLE

There are four path scanning methods being applied, it is noticeable that the raster and the snake scanning did not give any significant advantages of compression performance. As Table 14 shows, every scanning method gave almost the same compression ratio after applying the BWT and RLE. However the zig-zag scanning path gives the best overall result compared to the others.

Table 14: Predictive coding and different methods of BWT

Scan	GoldHill	Brigde	Boat	Barb	Birds	Airplane	Average
Zig-Zag	23.33	19.08	19.68	14.86	19.83	17.13	18.98
Hilbert	22.13	19.00	19.22	14.88	18.32	16.12	18.28
Raster	22.81	19.544	19.36	14.54	17.68	16.31	18.37
Snake	23.60	18.96	18.16	14.54	19.00	15.90	18.36

Chapter 6: Conclusions

In this thesis, the use of the Burrows-Wheeler transform in image compression was studied. A few discrete transformations, as well as predictive coding were considered. The difference of the quantization block sizes are presented and have been shown the results for the effect of the various block size of quantization table. Several linearization techniques were introduced to convert the 2-dimensional image to 1-dimensional linear data sequence. Also, variants of the Burrows-Wheeler transform methods have been considered.

The experimental results show that application the Burrows-Wheeler transformation gives a slightly improved performance on average compared to the JPEG standard. Also a combination of BWT with move-to-front and run-length encoding yield even better results when compared to JPEG standard. For linearizing the image a into linear pixel sequence by zig-zag scanning path after pre-processing with the discrete cosine transform gives the best result compared to the other scanning methods such as the raster, the snake or the Hilbert scanning path. Furthermore, the raster scan and the snake scan are competitive methods that were discovered while studying methods for linearizing the pixels sequence. As results show, the block size of 8×8 applying in

DCT will achieve a better result in the instance of using 2×2 , 4×4 , 16×16 , 32×32 or 64×64 block sizes. But the neighboring block size of 8×8 are gave quite good compression ratio compared to, for example, the block size of 2×2 and 64×64 . The Figure 18 showed the discrete cosine transform with different block sizes, visually the block size of 8×8 gave the best result for the reconstructed image.

The effect of using a different threshold will play an important role while processing a discrete wavelet transform. The experimental result shows that when tested the DWT with a higher threshold, the reconstructed image compression is better than in the case of a smaller threshold. This is noticeable from the pre-processing image, because the higher threshold will yield much more zeros at details coefficients of DWT. Scale 2 decomposition of DWT yields also a better compression ratio result, but on the other hand, the reconstructed image is poorer than by applying only scale 1 decomposition. For predictive coding, the uses of the Burrows-Wheeler transform and other variants of the BWT did not yield any better average results than applying only the predictive coding for image compression. The use of predictive coding after the Burrows-Wheeler transform as well as the move-to-front and the RLE was also tested. The result did not gave any better compression ratio compared to the predictive used before the Burrows-Wheeler transform. The use of a zig-zag scanning path gives also the best result in predictive coding as well as in DCT.

Generally, the use of Burrows-Wheeler Transform is suitable for image compression as well as others standard compression methods. When using discrete cosine transform with zig-zag scanning path and run-length coding, the result of compression ratio will even better than JPEG standard. On the other hand, one additional method causes an

extra execution time in the processors, because of the slowness in processing steps of BWT, which is a one of drawbacks when using this technique.

In the future the study will concentrate on different improvement algorithms of BWT to minimize execution time and the study of the compression in speech and video data using Burrows-Wheeler Transform.

References

- [1] Yun Q. Shi and Huifang Sun, Image and Video Compression for Multimedia Engineering, 2nd edition, *CRC Press, 2008*.
- [2] Khlid Sayood, Introduction to Data Compression, 2nd edition, *Morgan Kaufmann Publishers, CA, 2000*.
- [3] Donald Adjerob, Timothy Bell and Amar Mukherjee, The Burrows-Wheeler Transform: Data Compression, Suffix Arrays, and Pattern matching, *Springer, New York, 2008*.
- [4] R. C. Gonzalez and R. E. Woods, Digital Image Processing, 2nd edition, *Prentice Hall, New Jersey, 2002*.
- [5] R. C. Gonzalez, R. E. Woods, S. L. Eddins, Digital Image Processing Using Matlab, *Prentice Hall, New Jersey, 2004*.
- [6] Nandakishore R. Jalumuri, A Study of Scanning Paths for BWT Based Image Compression, Master's thesis, *Morgantown, West Virginia 2004*.
- [7] M. Burrows and D.J. Wheeler, A Block-sorting Lossless Data Compression Algorithm, *Research Report 124, System Research Center, Digital System Research Center, Palo Alto, CA, 1994*.

- [8] Ziya Arnavut and Spyros S. Megluveras, Block Sorting and Compression. *Data Compression Conference 1997: 181-190.*
- [9] Sanjiv K. Bhatia, Visual Data Processing, *Lecture note, May 2006.*
- [10] Paymen Zehtab Fard, Still Image Compression, *Lecture note, 1996.*
- [11] Ingela Nyström, Image Coding and Compression, *Centre for Image Analysis, Uppsala Universitet, November 2007.*
- [12] Kang-Hua Hsu, introduction to wavelet transform and image compression, *Graduate Institute of Communication Engineering, National Taiwan University, Taipei, Taiwan.*
- [13] Yao Wang, Wavelet Transform and JPEG2000, Polytechnic University, Brooklyn, NY 11201, USA
- [14] Sharon Shen, Discrete Wavelet Transform (DWT), *Lecture note, University of Maryland, Baltimore County, 2006*
- [15] Kharate, Patil and Bhale, Selection of Mother Wavelet For Image Compression on Basis of Nature of Image, *Journal of Multimedia, Vol. 2, No. 6, November 2007.*
- [16] Ayadi, Syiam and Gamgoum, Comparative Study of Lossy Image Compression Techniques, *IJCIS, Vol.6, No.1, January 2006.*
- [17] Arturo San Emeterio Campos, Run Length Encoding, *Arturo San Emeterio Campos, Barcelona 1999.*
- [18] Pizurica and Philips, Digital Image Processing, Ghent University, *Lecture notes in Computer science, January 2007.*
- [19] Subramanya and Youssef, Performance Evaluation of Lossy DPCM Coding of images Using Different Predictors and Quantizers, *ISCA CAINE98 Conference, Las Vegas, Nevada, November 1998.*

- [20] S. P. Nanavati and P. K. Panigrahi, Wavelet: Application to Image Compression-II, *Springer India, in co-publication with Indian Academy of Sciences, Volume 10, Number 3 / March, 2005*
- [21] Mariusz Jankowski, Digital Image Processing, *Mathematica Second Edition Published by Wolfram research, 2007*
- [22] A Mathematical Theory of Communication, C. E. Shannon, *The Bell System Technical Journal, Vol. 27. pp. 379-423, 623-656, July, October, 1948*
- [23] Ping-Sing Tsai and Tinku Acharya, Image Up-Sampling Using Discrete Wavelet Transform, *JCIS-2006 Proceedings, October 2006*
- [24] Oge Marques, Image Compression and Coding, Department of Computer Science and Engineering, *Florida Atlantic University, Boca Raton, FL, USA*
- [25] Myllyoja Jani, Burrows-Wheeler-pakausmenetelmä ja sen variaatiot, Master's Thesis, *Turku University, Summer 2003*
- [26] Mauro Barmis, Document and image compression, *CRC Press, USA, 2006*

Appendix A

There are 7 test images used in this thesis, images are *GoldHill*, *Bridge*, *Boat*, *Women*, *Birds*, *Airplane* and *Lena*. The test images are from <http://decsai.ugr.es/cvg/CG/base.htm>.

GoldHill



Bridge



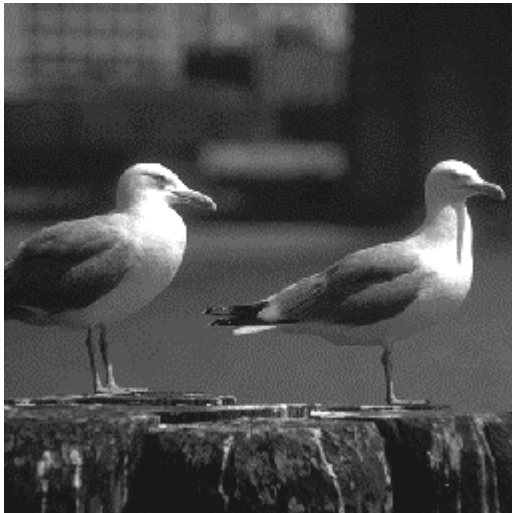
Boat



Barb



Birds



Airplane



Lena

